# Distribution and behaviour of naturally occurring radionuclides within a Scots pine forest grown on a $CaF_2$ waste deposit related to the Belgian phosphate industry

Nathalie Vanhoudt[1*], Axel Van Gompel[1], Jordi Vives i Batlle[1]

[1]Biosphere Impact Studies, Belgian Nuclear Research Centre (SCK CEN), Boeretang 200, 2400 Mol, Belgium

[*]Corresponding author: nathalie.vanhoudt@sckcen.be

***Abstract***

The distribution and behaviour of naturally occurring radionuclides within a vegetated part of a $CaF_2$ sludge heap from the Belgian phosphate industry was studied. A Scots pine forest plot was selected as study area. Trees were approximately 20 years old and showed a disturbed health state. Seasonal sampling campaigns of soil, roots, wood, inner and outer bark, needles and twigs gave insight on $^{238}U$, $^{226}Ra$, $^{210}Pb$ and $^{210}Po$ transfer and distribution between pine tree compartments. Soil samples were analysed for their texture, total organic and inorganic carbon, field capacity, pH and radionuclide content. Solid-liquid distribution coefficients ($K_d$) were experimentally determined for $^{238}U$, $^{226}Ra$ (using Ba as analogue) and $^{210}Pb$ based on adsorption-desorption batch tests.

Results indicated higher $^{238}U$, $^{232}Th$, $^{226}Ra$, $^{210}Pb$ and $^{210}Po$ activity concentrations in the deeper soil layers while the first 20 cm contained less radionuclides but had a higher level of organic carbon. Additionally, results indicated no seasonal changes in the $^{238}U$:$^{226}Ra$ ratio in the soil while the $^{226}Ra$:$^{210}Pb$ ratio was significantly higher in spring compared to winter in the 20-60 cm soil layer. Pine tree roots served as natural translocation barrier for all radionuclides with high retention in the roots and low translocation to the above ground tree compartments. When considering the above ground

compartments, $^{210}$Pb and $^{210}$Po were mostly present in the bark, needles and twigs. Furthermore, $^{238}$U and its progeny were highly accumulated in mosses. These results allowed us to establish more realistic soil-to-plant transfer factors. In addition, experimentally mimicking pore water acidification in the root zone resulted in lower $^{238}$U and $^{210}$Pb $K_d$ values compared to using a standard $CaCl_2$ solution.

This study provides an integrated radioecological picture of knowledge and site specific data needed to study the long-term influence of vegetation on radionuclide dispersion in forest ecosystems.

***Keywords***

Isotopic ratio, radionuclide cycling, seasonal variation, solid-liquid distribution coefficient, terrestrial ecosystem, transfer factor

## 1. Introduction

Several industries are involved in the extraction or processing of materials containing enhanced levels of naturally occurring radionuclides including the primordial radionuclides $^{238}U$, $^{232}Th$ and their decay products $^{226}Ra$, $^{210}Pb$ and $^{210}Po$ (EC, 2001). The most contaminating and widely distributed of these type of industries includes uranium mining and milling, metal mining and smelting, and the phosphate industry (Vandenhove et al., 1999). The European phosphate industry for example, uses mainly ores from Moroccan origin containing $^{238}U$ and $^{226}Ra$ activity concentrations between 1.5 and 1.7 kBq $kg^{-1}$ (Vandenhove et al., 1999). This will result in increased $^{238}U$ and/or $^{226}Ra$ concentrations in the produced fertilisers, phosphogypsum and waste products, leading to enhanced radionuclide levels in the environment (IAEA, 2013). These radionuclides can be further dispersed in the environment, entering soils, surface- and groundwater, bioaccumulating in food webs, causing adverse effects on biota and posing severe risks to human and ecosystem health (Gall et al., 2015). However, risks to human health and the environment can also come from non-radioactive constituents such as fluorides and metal(loid)s (e.g. As, Cd, Pb and Hg) which are also related to the phosphate industry and are usually of primary importance compared to radiological considerations (IAEA, 2013).

Forest ecosystems play an important role in the cycling of elements and radionuclides in the environment. Radionuclides can be efficiently trapped and recycled in forests leading to long residence times and an enhanced risk for internal and external exposure to people and wildlife (IAEA, 2009). For example, recycling of $^{137}Cs$ present in forests resulting from the Chernobyl and Fukushima accidents, occurred as a dynamic process in which $^{137}Cs$ is transferred between biotic and abiotic components on a seasonal or longer term basis (IAEA, 2002; Thiry et al., 2009; Yoschenko et al., 2017). Scots pine trees (*Pinus sylvestris* L.) are distributed worldwide and make an important constituent of European forests (Mason and Alía, 2000). Research towards their role in element cycling in forest ecosystems with regard to ecosystem functioning has been performed in the past (Gielen et al., 2016; Helmisaari, 1995). Moreover, many studies have been performed to increase our understanding of the biogeochemical cycling of radionuclides in forest ecosystems through experiments and the application of mathematical

models (Goor and Thiry, 2004; IAEA, 2002; Thiry et al., 2020; Van den Hoof and Thiry, 2012). Research during the last decades was predominantly related to accident scenarios focussing on $^{137}Cs$ and $^{90}Sr$ (Endo et al., 2015; IAEA, 2009; Thiry et al., 2009). Nonetheless, several studies exist on the distribution of naturally occurring radionuclides in vegetation (including Scots pine trees) grown on contaminated sites related to uranium mining and the phosphate industry (Charro and Moyano, 2017; Corisco et al., 2017; Strok et al., 2011).

Since a century, the phosphate industry has been an important industrial activity in Belgium for the production of phosphoric acid, fertilisers and cattle food (Paridaens and Vanmarcke, 2008). In this specific case, hydrochloric acid was used for the acidulation of phosphate ores of Moroccan origin which contained trace levels of metals and naturally occurring radionuclides from the $^{238}U$ and $^{232}Th$ decay series. As a result of the chemical processing, a sludge of mainly insoluble $CaF_2$ was produced and deposited as waste product from 1945 until 1979. This sludge contained $^{226}Ra$ activity concentrations up to 4 kBq $kg^{-1}$ and gamma dose rates of 1 µSv $h^{-1}$ were measured according to Paridaens and Vanmarcke (2008). While activities are ongoing on a certain part of the site, another part of the site is currently not being used and covered with 20-year-old Scots pine trees in addition to other vegetation such as birch trees, grasses, shrubs, etc. Elevated levels of $^{238}U$, $^{232}Th$, $^{226}Ra$, $^{210}Pb$ and $^{210}Po$ can be found in the sludge and in the vegetation grown on this contaminated substrate. In addition, elevated concentrations of metals and metalloids such as As, Cd, Cr, Pb and Zn are also present. This historical contaminated site provides a unique research location due to the mixed nature of the contamination and the growth of a variety of vegetation on the unconventional growth substrate $CaF_2$. The site development as a radioecological observatory was driven by the need to improve current models that describe radionuclide behaviour in the environment with site specific data and to facilitate other research initiatives. The process was initiated under EC-projects STAR and COMET as an observatory site to ensure joint, long-term radioecological research. It was then further developed by adding an instrumented forest plot under the EC-TERRITORIES project

85 (https://territories.eu/) to support research on processes with an eye to reduce modelling
86 uncertainties (https://radioecology-exchange.org/content/belgian-norm-site).

87 Within the present study, it was our objective to gain in-depth mechanistic knowledge and acquire
88 high-quality site specific data on the distribution and behaviour of naturally occurring radionuclides
89 ($^{238}U$, $^{232}Th$, $^{226}Ra$, $^{210}Pb$ and $^{210}Po$) in a pine forest grown on a $CaF_2$ sludge heap related to the phosphate
90 industry. The obtained data and insights will allow researchers to better understand and model the
91 long-term influence of vegetation on radionuclide dispersion in forest ecosystems and to gain more in-
92 depth knowledge on processes determining radionuclide mobility and bioavailability in soil and
93 especially $CaF_2$ sludge.

## 2. Material and methods

### *2.1 Selection of forest plot*

A systematic approach was used to select an appropriate forest plot with Scots pine trees (*Pinus sylvestris*) on the $CaF_2$ waste heap. The work was performed on an area of approximately 7 ha of the sludge heap which was naturally revegetated and made available for scientific research activities by the site owner (Fig. 1 – area outlined in red).

The accessibility of the site was visually evaluated together with the variability of plant species. The vegetation growing on the site included 20-year-old Scots pine trees (*Pinus sylvestris*), birch trees (*Betula pendula*), American oak (*Quercus ruba*), grasses, herbs (e.g. *Eupatorium cannabinum*, *Tanacetum vulgare*, *Tussilago farfara*), reed (*Phragmites australis*, *Calamagrostis epigejos*), etc. The areas with Scots pine trees as the dominant vegetation were identified. The spatial variability of the radionuclide distribution at the site was mapped by measuring the gamma dose rate at 1 m above the ground using an Automess 6150 gamma dose rate detector combined with an Automess scintillator probe 6150AD. We covered the area spatially with the aid of a coupled GPS system. From the dose rate map (Fig. 2) it was clear that the contamination was heterogeneously distributed over the site. This was an important source of uncertainty as relatively high contamination areas were close to lower level areas, with the presence of occasional hotspots. The map was therefore used as a guide to select an area where the contamination was expected to be relatively elevated, although local variability in contamination levels was not available. Based on the gamma dose rate map and a visual inspection regarding accessibility and dominant vegetation type, three areas of interest could be distinguished (Fig. 1 – areas outlined in blue).

Pine trees in these three plots were visually inspected for their age and general health status. The trees appeared to be less healthy than in non-contaminated areas. We hypothesise that this poor health could be due to low soil nutrient content, limited extractability of water from the sludge and the presence of chemical pollutants, with radioactive contamination being the least likely deleterious

119 influence. In general, the trees were estimated to be around 20 years old although they were shorter
120 than expected. Branches started very close to the ground instead of 2 m above ground. Tree trunks
121 were often not straight and the height increment between branches was in the order of 0.5 m instead
122 of 1 m, all signs of pour health and distress (Fig. 3A) (Vincke, 2018, personal communication).

123 From the three areas of interest, two areas were rejected because (a) they appeared to be recently
124 disturbed, (b) they had excessively mixed vegetation, (c) there were trenches along the borders which
125 could influence the water balance inside the plot or (d) the health of the trees was unrepresentatively
126 poor. The chosen area (Fig. 1 – green area) was located in a relatively high contaminated spot (Fig. 2)
127 with uniformly spread vegetation dominated by Scots pine trees with a somewhat healthier
128 appearance compared with the worst affected areas. The lower tree branches were also farther from
129 the ground, facilitating the installation of sap flow sensors in a later phase. The heterogeneity of the
130 vegetation in terms of morphological and age differences between Scots pine trees was another source
131 of uncertainty. Determining the circumferences of 100 Scots pine trees at a height of approximately
132 1.3 m above ground helped us to identify trees belonging to the same age class. Scots pine trees at the
133 chosen area had an average circumference of 46 ± 1 cm.

134 Based on this information, we pinpointed the optimum location to characterise the soil and to follow
135 the distribution of radionuclide concentrations between pine tree compartments, moss and soil within
136 different seasons. This study plot had a diameter of about 16 m (Fig. 1 – marked with a yellow star).

137 *2.2 Soil characterisation*

138 To characterise the growth substrate (soil/sludge) in the study area, samples were taken at 4 locations
139 distributed within this area[1]. After carefully separating the moss or litter fall, samples were taken at 3
140 depths: 0-20 cm, 20-60 cm and 60-100 cm. Samples were air-dried, grounded and sieved (2 mm) before
141 analysing their characteristics. Texture (% sand (50-2000 µm), % silt (2-50 µm), % clay (<2 µm)) were

[1] The growth substrate of the vegetation is referred herein as "soil" for simplicity reasons. However, in reality, the site contains $CaF_2$ sludge covered by some 20 cm of organic soil.

142 determined based on the ISO 11277:1998 international standard (ISO, 1998). Total organic and
143 inorganic carbon were determined using a TOC-L CPH analyzer with SSM-5000A Solid Sample Module
144 (Shimadzu Deutschland GmbH, Germany). Samples were grinded, dried at 105 °C, and $V_2O_5$ was added
145 as catalyst to convert the total carbon to $CO_2$ by combustion at 900 °C in an oxygen gas flow. The
146 oxygen gas carried the released $CO_2$ to a non-dispersive infrared gas analyser. The total carbon content
147 could be determined based on a calibration curve using glucose and acetanilide as standards. The total
148 organic carbon content was determined by measuring the total carbon content after removal of all
149 inorganic carbon in the grinded and dried samples via a hydrochloric acid treatment. The total
150 inorganic carbon was calculated as the difference between the total carbon and total organic carbon
151 concentration. The field capacity was derived with the saturated paste method and calculated as 50 %
152 of the water content of saturated paste (Rhoades, 1982). In addition, samples were analysed for pH-
153 $H_2O$ (1/2.5 solid/liquid).

154 The activity concentrations of $^{238}U$, $^{232}Th$, $^{226}Ra$ and $^{210}Pb$ in the samples were determined by high
155 resolution gamma-ray spectroscopy using HPGe detectors at the Belgian Nuclear Research Centre,
156 which operates under the ISO17025 standard. The calculation of the activity was performed with the
157 Genie2K program in combination with a LIMS-system. Corrections for efficiency transfer and summing
158 were calculated with the EFFTRAN program (http://efftran.com/). The efficiency curve was made with
159 a certified multi gamma solution ($^{210}Pb$, $^{241}Am$, $^{113}Sn$, $^{51}Cr$, $^{57}Co$, $^{137}Cs$, $^{60}Co$, $^{58}Sr$, $^{139}Ce$, $^{109}Cd$, $^{88}Y$) in
160 different geometries. The relative efficiency of the detectors was found to be between 38 and 50 %.
161 The energy resolution was 0.8 keV at 46 keV and about 1.8 keV at 1460 keV. Density corrections for
162 the matrix were performed. The nuclear data used for the determination of radionuclides and the
163 activity calculation came from the recommended database of LNHB: www.lnhb.fr/nuclear-data.
164 Equilibrium was assumed between $^{238}U$ and its daughter radionuclides when the daughters were used
165 for the activity calculation of the mother ($^{238}U$, $^{232}Th$ and $^{226}Ra$). For $^{226}Ra$ determination, the sample
166 was air tightened to avoid escape of the volatilised $^{222}Rn$ daughter of $^{226}Ra$, essential to avoid isotopic
167 ratio distortions when using this method.

The effects of depth, pH, and total organic carbon on the activity concentration of $^{238}U$, $^{226}Ra$ and $^{210}Pb$ were tested with linear mixed effects models (Verbeke and Molenbergs, 2000) using the freeware software package R (R Development Core Team, 2011). We used a top-down approach in which non-significant parameters were removed step-by-step. Differences in soil characteristics (pH, total organic carbon, total inorganic carbon and field capacity) between depths were statistically evaluated using one-way analysis of variance and Tukey multiple comparison testing. Multivariate analysis of variance on isometric log ratio transformed values was used to evaluate the change of soil texture with depth.

### *2.3 Solid-liquid distribution coefficients*

The solid-liquid distribution coefficients ($K_d$ – Eq. 1) of radionuclides ($^{238}U$, $^{226}Ra$ and $^{210}Pb$) in the sludge layer below 20 cm can be derived from the solid-liquid distribution of soil-borne radionuclides (present in the sludge) or from the solid-liquid distribution of added radionuclides (or stable isotopes).

$$K_d = \frac{Activity\ concentration\ in\ solid\ phase\ [Bq\ kg^{-1}]}{Activty\ concentration\ in\ liquid\ phase\ [Bq\ L^{-1}]} \quad \text{(Eq. 1)}$$

First, to derive $K_d$ values based on the radionuclides already present in the sludge, pore water was extracted from 6 sludge samples (taken at a depth below 20 cm). Sludge samples were brought to field capacity and after an equilibration time of 3-4 weeks, pore water was separated by centrifugation (6000 rpm, 30 min) and filtered (0.45 µm syringe filter). The activity concentrations of $^{238}U$, $^{226}Ra$ and $^{210}Pb$ in the pore water were determined using high resolution gamma-ray spectroscopy. $^{232}Th$ activity was not measured in the pore water as this was already expected to be below the detection limit, based on the measured $^{232}Th$ activity concentration in sludge samples. The radionuclide activity concentrations in the solid phase were measured directly on dried samples, as previously described.

Next, one sludge sample taken at a depth of 60-100 cm was used to derive $K_d$ values for $^{238}U$, stable Pb and stable Ba (as analogue for $^{226}Ra$) using an adsorption-desorption batch test with addition of radionuclides (or stable isotopes or analogues) based on OECD (2000). As a first step, small amounts of dried and sieved sludge were equilibrated overnight by shaking with 95 % volume of the liquid

phase. For the liquid phase, 0.01 M $CaCl_2$ or 0.1 M citric acid – sodium citrate buffer (pH 5 – to mimic the acidification of the root zone) was used. Next, 5 mL of the spiked solution was added and the mixture was shaken for 7 days. Afterwards, the sludge suspensions were separated by centrifugation (4800 rpm, 10 min), followed by filtration through a 0.45 µm syringe filter which was then analysed for the element of interest. The amount of element adsorbed on the sludge sample was calculated as the difference between the amount initially present in the solution and the amount remaining at the end of the test. Each experimental condition was set up in duplicate. For $^{238}U$, 0.5 g sludge was brought in contact with 250 mL solution (0.01 M $CaCl_2$ or 0.1 M citric acid – sodium citrate buffer (pH 5)), spiked with 6800 Bq $L^{-1}$ $^{238}U$ in $UO_2(NO_3)_2.6H_2O$. For Pb, 0.2 g sludge was brought in contact with 100 mL solution (0.01 M $CaCl_2$ or 0.1 M citric acid – sodium citrate buffer (pH 5)) spiked with 30 mg $L^{-1}$ Pb in $PbNO_3$. As Ba was already present in the sludge at elevated concentrations, there was no need to additionally spike the solution and Ba concentrations were measured in the sludge and solutions from the Pb-tests. The remaining $^{238}U$ activity in the liquid phase was measured using high resolution gamma-ray spectroscopy, whilst Pb and Ba concentrations were determined using Microwave Plasma Atomic Emission Spectroscopy (MP-AES). The Ba content in the sludge was analysed with ICP-AES after a microwave digestion using $HCl/HNO_3/HBF_4$.

### *2.4 Distribution of naturally occurring radionuclides in soil, moss and pine tree compartments*

Sampling campaigns were organised during fall (November 2017), winter (February 2018), spring (May 2018) and summer (August 2018) to evaluate the distribution of radionuclides in soil, moss and pine tree compartments. During each sampling campaign, three trees were felled with a circumference of 30.8 ± 1.9 cm at 1.3 m height. A piece of 1 m length was cut from each trunk between 50 and 150 cm above the ground. The trunks were separated into wood (= sapwood + heartwood), inner bark and outer bark as described in Gielen et al. (2016). In addition, we took samples of soil (0-20 cm and 20-60 cm), roots (mixture of fine and coarse roots up to 60 cm depth) and moss. Activity concentrations of $^{238}U$, $^{232}Th$, $^{226}Ra$ and $^{210}Pb$ were measured in these samples using high resolution gamma-ray spectroscopy (see Section 2.2). Detection limits were computed according to the ISO 11929:2010

218 international standard with α = β = 5 % (ISO, 2010). $^{232}$Th measurements are not shown for tree
219 compartments and moss as these did not reach the detection limit. The $^{210}$Po content was determined
220 in soil and vegetation samples using high resolution alpha spectrometry after chemical separation and
221 electrodeposition.

222 No statistical analyses were performed to evaluate the seasonal changes on radionuclide activity
223 concentrations in the different tree compartments because activity concentrations often did not reach
224 the detection limits. Also for moss, no statistical analyses were performed due to the limited number
225 of replicates. Given the heterogeneous radionuclide contamination of the site, there was also no added
226 value in statistically evaluating the seasonal variation of the soil radionuclide content. However,
227 seasonal variation in the $^{238}$U:$^{226}$Ra and $^{226}$Ra:$^{210}$Pb ratios could be evaluated based on the 0-20 cm and
228 20-60 cm soil samples using one-way analysis of variance and Tukey multiple comparison testing with
229 the freeware software package R (R Development Core Team, 2011). The normality assumption was
230 tested using the Shapiro-Wilk test. In addition, the same statistical approach was used to evaluate
231 differences in radionuclide activity concentration between tree compartments and between the upper
232 and lower soil layer with the data combined for all the seasons.

233 *2.5 Soil-to-plant transfer factors*

234 The activity concentrations of $^{238}$U, $^{226}$Ra, $^{210}$Pb and $^{210}$Po in the whole tree could be calculated based
235 on the activity concentrations measured in the different tree compartments and derived mass
236 weighting factors for these compartments according to Xiao and Ceulemans (2004) and Ukonmaanaho
237 et al. (2008) (Eq. 3). For this purpose, the samples from the four seasons were combined to increase
238 the statistical power of the calculations. $^{232}$Th was not included as the concentrations in the soil and
239 tree compartments were too low and could often not reach the detection limit.

240 $$C_{tree} = 0.191 \times C_{roots} + 0.53 \times C_{wood} + 0.059 \times C_{bark} + 0.22 \times C_{needles} \quad \text{(Eq. 3)}$$

241 Where $C_{tree}$ is the activity concentration of the radionuclides in the whole tree [Bq kg$^{-1}$], $C_{roots}$ the
242 activity concentration of the radionuclides in the roots [Bq kg$^{-1}$], $C_{wood}$ the activity concentration of the

243 radionuclides in the wood (= sapwood + heartwood) [Bq kg$^{-1}$], $C_{bark}$ the activity concentration of the
244 radionuclides in the inner and outer bark [Bq kg$^{-1}$] and $C_{needles}$ the activity concentration of the
245 radionuclides in the needles and twigs younger or older than 1 year [Bq kg$^{-1}$]. $C_{bark}$ was calculated
246 assuming a 1:1 mass ratio for inner and outer bark. Although this ratio is less than 1 for older trees
247 according to Gielen et al. (2016), using a 1:1 ratio is more appropriate for the younger trees we
248 sampled.

249 We calculated soil-to-plant transfer factors for trees and mosses based on Eq. 4.

250 $$TF = \frac{C_{plant}}{C_{soil}} \quad \text{(Eq. 4)}$$

251 With *TF* the soil-to-plant transfer factor [-], $C_{plant}$ the radionuclide activity concentration in the plant
252 [Bq kg$^{-1}$] and $C_{soil}$ the radionuclide activity concentration in the soil [Bq kg$^{-1}$].

253 The samples from the four seasons were combined to make these calculations. The soil-to-moss
254 transfer factors were calculated based on the radionuclide activity concentrations in the upper soil
255 layer (0-20 cm). For pine trees, the reference activity concentrations in the soil were calculated based
256 on the relative distribution of the pine tree roots in the soil. An exponential root model was used to
257 calculate the expected fraction of roots in the 0-20 cm soil layer (Li et al., 1999; 2001; 2006). This
258 assumes that the root system has exponentially decreasing density distribution with depth z, down to
259 a maximum rooting depth (Eq. 5).

260 $$RD(z) = RD_0 \left[1 - \frac{1}{1+e^{-bz}} + \frac{1}{2}e^{-bz}\right] \quad \text{(Eq. 5)}$$

261 Where $RD_0$ is the root density at $z$ = 0 and $b$ is an empirical 'root extinction coefficient', reported to be
262 10 m$^{-1}$ for various plants with a shallow root distribution in clay soil such as it would be for coniferous
263 woodland (Dwyer et al., 1988).

264 As such, the model predicted that 84 % of the roots was present in the 0-20 cm layer, in agreement
265 with reported root density profiles for Scots pine trees by Vincke and Thiry (2008). We assumed the

266 remaining 16 % of the roots to be in contact with the >20 cm soil having a uniform radionuclide activity

267 concentration, as justified by the data in Fig. 4.

## 3. Results and discussion

### *3.1 Soil characterisation*

The sludge on the site was relatively impermeable and covered by approximately 10 to 20 cm of a more organic top-layer (Fig. 3B). Indeed, a significantly higher organic carbon content could be measured in the first 20 cm layer compared to the lower sludge (Table 1). From the texture determinations, it was observed that approximately 60 % could be considered clay type material with only a small fraction of sand (Table 1). This texture was completely different from the sandy soils on which pine trees prefer to grow. This can be illustrated by a soil texture of 91.7 % sand, 7.1 % silt and 1.2 % clay in the 23-110 cm layer, reported by Vincke and Thiry (2008), for a Scots pine forest planted in 1949 approximately 25 km North from the sludge heap. Consequently, the sludge acted as a rather impermeable layer, accumulating water in winter and slowly drying in summer by evapotranspiration. During very dry periods (summer time), we observed that the sludge was more compact and cracks of several centimetres wide and up to several decimetres deep appeared, owing to the water loss. Furthermore, no significant differences were observed for the field capacity or pH in function of depth (Table 1). A pH-$H_2O$ of approximately 7.2 was measured for the $CaF_2$ sludge on which the pine trees were growing. This is much higher than the pH-$H_2O$ of approximately 4.7 measured in the soil of a regular Belgian pine tree forest (Vincke and Thiry, 2008).

In addition to determining soil characteristics over the study area, the uncertainty related to the heterogeneity of the soil was also addressed by measuring the radionuclide activity concentrations of $^{238}U$, $^{232}Th$, $^{226}Ra$ and $^{210}Pb$ in these soil samples. Fig. 4 illustrates that the activity concentrations of these radionuclides were significantly lower in the top 20 cm layer compared to the lower sludge layers. $^{232}Th$ is not shown in Fig. 4 due to the low activity concentrations of 46 ± 1, 54 ± 3 and 57 ± 6 Bq $kg^{-1}$ in the 0-20 cm, 20-60 cm and 60-100 cm layer respectively. However, the $^{232}Th$ activity concentration in the top soil layer was also significantly lower compared to the deeper layers. Although activity concentrations of $^{210}Po$ were not measured in the 60-100 cm soil layer, $^{210}Po$ activity

concentrations were shown to be significantly higher in the 20-60 cm soil layer compared to the 0-20 cm soil layer (Table 3). Based on current knowledge of the site and soil analyses made, we hypothesise that the difference in activity concentration with depth could, at least partly, be explained by the difference in composition of the top layer compared to the lower sludge layers. Indeed, the top layer is made of litter fall and decayed organic material generated over years and mixed with the top sludge layer, creating a more organic mulch that contains less radioactivity. This could be related to dilution of the radionuclides by the newly formed material and/or the formation of more leachable organic compounds. While other mechanisms might also contribute to explain the vertical distribution of the radionuclides in the soil, current data do not allow us to draw solid conclusions.

As a consequence of the specific production process applied on the phosphate ores, $^{238}U$ and $^{226}Ra$ were no longer in secular equilibrium in the waste streams. Due to the relatively short life-span of the waste deposit (waste deposited from 1945 until 1979), no secular equilibrium could be expected between $^{238}U$ and its daughters or between $^{226}Ra$ and its daughters as illustrated by a $^{238}U$:$^{226}Ra$ activity ratio of 1.39 ± 0.02 and a $^{226}Ra$:$^{210}Pb$ activity ratio of 1.49 ± 0.06 for the 20-60 cm layer, instead of a ratio of 1 in the case of secular equilibrium. Moreover, the $^{226}Ra$:$^{210}Pb$ (or $^{226}Ra$:$^{210}Po$) activity ratio can also change (especially in the top 1 m of the soil) due to the exhalation of $^{222}Rn$ (IAEA, 2017). $^{210}Po$ on the other hand seemed to be in equilibrium with its parent $^{210}Pb$ with a $^{210}Pb$:$^{210}Po$ ratio of 1.1 ± 0.2. This could be expected as $^{210}Pb$ and $^{210}Po$ can reach equilibrium after approximately 2 years (Bonczyk, 2013).

*3.2 Radionuclide distribution between liquid and solid phase*

The mobility of radionuclides in soils is strongly determined by their sorption behaviour on the solid phase and is often quantified by the empirical solid-liquid distribution coefficient ($K_d$). Although simple to measure and to use in radiological impact assessments, $K_d$ values have a high variability (several orders of magnitude) that can be attributed to soil mineralogy, organic matter, soil geochemistry, radionuclide speciation, time after contamination, or the system not being at equilibrium (Vandenhove

et al., 2009a). Site specific $K_d$ values are therefore advised when performing impact assessments, although the large number of experimental approaches will also lead to $K_d$ values that express partitioning between different pools and as such a wide variation in obtained $K_d$ values (Degryse et al., 2009; EPA, 1999).

Two experimental approaches were applied to obtain specific $K_d$ values for the naturally occurring radionuclides present in the $CaF_2$ sludge. Within the first approach, we intended to determine the total $K_d$ of the soil-borne radionuclides in the soil in which soil aging is taken into account that can lead to a fraction of radionuclides that are irreversibly sorbed to the solid phase (Degryse et al., 2009; IAEA, 2009). Radionuclide concentrations were directly measured in the soil and the extracted pore water. However, the sludge acted as a very strong sorbent for these radionuclides and concentrations in the liquid phase were below the detection limit (results not shown) making it not possible to calculate total $K_d$ values.

In addition, standard adsorption-desorption batch tests were performed with spiked solutions to determine the exchangeable or labile $K_d$ for $^{238}U$, stable Pb and stable Ba as analogue for $^{226}Ra$. This labile $K_d$ represents the process in which the radionuclide is reversibly sorbed to the solid phase (Degryse et al., 2009). When using a standard 0.01 M $CaCl_2$ solution as liquid phase, a $K_d$ value of (4.7 ± 0.1) × $10^4$ L $kg^{-1}$ could be calculated for $^{238}U$ (Table 2). This value was in the upper range of $K_d$ values reported for $^{238}U$ in different soil types ranging from 0.7 to 6.7 × $10^4$ L $kg^{-1}$ when considering all soil types but different when considering pH as a cofactor criterion (0.9 to 6.2 × $10^3$ L $kg^{-1}$ for pH ≥ 7) (IAEA, 2010). Based on its texture (Table 1), the $CaF_2$ substrate could be classified under clay soils. However, when comparing the obtained $^{238}U$ $K_d$ value with the ones reported for clay soils, it did not fall within the reported range of 3 to 480 L $kg^{-1}$ (Vandenhove et al., 2009a). Although the reported range was derived from a limited amount of measurements, it indicates that caution is needed when using literature $K_d$ values for substrates different from soil. A $K_d$ value of (4.7 ± 0.2) × $10^5$ L $kg^{-1}$ was obtained for Pb when using a 0.01 M $CaCl_2$ solution as the liquid phase (Table 2). This was higher than the $K_d$

343 values reported for Pb in different soil types, ranging from 25 to $1.3 \times 10^5$ L $kg^{-1}$ (IAEA, 2010). The
344 elevated levels of Ba present in the sludge were used to determine its $K_d$ value which can be considered
345 as an analogue for $^{226}Ra$ (IAEA, 2014). A $K_d$ value of $(4.7 \pm 0.8) \times 10^2$ L $kg^{-1}$ could be calculated (Table 2)
346 which was in the lower range of previously summarised $K_d$ values for Ra ranging between 12 and $9.5 \times$
347 $10^5$ L $kg^{-1}$ for all types of soil (IAEA, 2010).

348 Root-mediated changes of pH can occur in the rhizosphere and can influence the bioavailability of
349 nutrients and toxic elements (Hinsinger et al., 2003). Acidification of the near vicinity of the roots is
350 dependent on a range of internal and regulatory processes but can also be related to environmental
351 stresses such as nutrient deficiencies and metal toxicities (Hinsinger et al., 2003). Based on the
352 substrate's pH and environmental stresses (e.g. presence of toxic metals) the pine trees were exposed
353 to, we assumed that the roots of the trees can locally acidify the soil, leading to an increased
354 bioavailability and root uptake of the radionuclides. Therefore, additional $K_d$ values were determined
355 using a 0.1 M citric acid – sodium citrate buffer at pH 5 to mimic the rhizosphere. Together with oxalic
356 and malic acids, citric acid is present in root cells and often referred to for its potential effect on the
357 rhizosphere (Hinsinger et al., 2003). In the case of *Pinus sylvestris*, Magdziak et al. (2020) illustrated
358 the presence of various aliphatic low molecular weight organic acids in the rhizosphere and showed
359 that elevated metal levels in the soil could induce citric acid secretion. Our measurements indicated
360 that when using the citric acid – sodium citrate buffer as liquid phase, the obtained $K_d$ for $^{238}U$ was
361 approximately 150 times lower compared to the $K_d$ using a standard 0.01 M $CaCl_2$ solution as liquid
362 phase (Table 2). This is in line with a study from Duquène et al. (2008) in which the effect of
363 biodegradable amendments was tested on the U solubility in soils. Addition of citric acid or an $NH_4^+$-
364 citrate/citric acid mixture to U contaminated soil highly increased the U concentration in the soil
365 solution after 7 days, leading to a 4 to 254 decrease in $K_d$ values depending on the soil type (Duquène
366 et al., 2008). The pH of the environment will influence the U speciation, which determines its solubility
367 and bioavailability (EPA, 1999). As such, $K_d$ values of U will show a specific trend in relation to the pH
368 as reported by Vandenhove et al. (2009a). Moreover, for Pb, our results show a high reduction of

experimentally determined $K_d$ values with a factor 3000 when 0.1 M citric acid – sodium citrate buffer was used as liquid phase (Table 2). A number of studies indicate a relationship between Pb $K_d$ and pH with increasing $K_d$ if pH increases as summarised by EPA (1999). When classifying literature $K_d$ values for Pb based on soil pH, Vandenhove et al. (2009a) reported 20 times lower $K_d$ values for pH values between 3 and 6.4, compared to higher pH values. Ba $K_d$ values on the other hand, did not change when using 0.1 M citric acid – sodium citrate buffer as liquid phase compared to 0.01 M $CaCl_2$ (Table 2). Although adsorption processes for Ra are pH dependent (IAEA, 2014), pH could not be suggested as a suitable parameter for classifying Ra $K_d$ values according to Vandenhove et al. (2009a).

*3.3 Distribution of naturally occurring radionuclides in soil, moss and pine tree compartments*

3.3.1. Uncertainties related to seasonal variation of naturally occurring radionuclides

Seasonal data on $^{238}U$, $^{226}Ra$ and $^{210}Pb$ content of soil, moss and pine tree compartments (roots, bark, wood, needles and twigs) are summarised in Tables 3, 4 and 5. Samples taken at one growth season (spring or summer) were additionally analysed for their $^{210}Po$ content (Tables 3, 4 and 5). Although the data are presented subdivided per season, it is not possible to make strong statements related to seasonal variability of the radionuclide content of the samples as there is not enough statistical significance to back-up the perceived variations.

Ultimately, the variability of the soil radionuclide content relates to the heterogeneity of the contamination on the site. This heterogeneity, although limited in the small sampling area used in this study, did not allow to deduce clear season-induced alterations in soil radionuclide content. However, as $^{238}U$, $^{226}Ra$ and $^{210}Pb$ concentrations were always measured together in each soil sample, it was possible to evaluate seasonal variations in the $^{238}U$:$^{226}Ra$ and $^{226}Ra$:$^{210}Pb$ ratios in the soil. There were no significant differences in the $^{238}U$:$^{226}Ra$ ratio between the different seasons both for top (0-20 cm) and lower (20-60 cm) soil layers (Table 3). The radionuclides were already present in the sludge when dumped on the site and no extra external input of radionuclides occurred. Moreover, leaching was not considered to significantly contribute to the seasonal variability in radionuclide concentration in the

394 soil as leaching was expected to be limited based on results from previously performed leaching studies
395 on the sludge samples (Site owner, 2015, personal communication). In addition, $^{226}$Ra:$^{210}$Pb ratios were
396 calculated for the different seasons in the 0-20 cm and 20-60 cm soil layers (Table 3). Statistical
397 analyses of these data indicated a significant difference between the $^{226}$Ra:$^{210}$Pb ratios for winter and
398 spring in the lower soil layer. We hypothesise that this difference is partly due to seasonal variations
399 in radon exhalation from soil, although more measurements are necessary to extract firm conclusions.
400 Radon exhalation rates from soil are indeed dependent on weather conditions (e.g. rainfall and
401 temperature) in addition to geophysical and geochemical characteristics of the substrate (Karstens et
402 al., 2015; López-Coto et al., 2013). When comparing the $^{226}$Ra:$^{210}$Pb ratio over all seasons in the lower
403 soil layer (20-60 cm) with the top layer (0-20 cm), a significantly higher ratio could be observed in the
404 top layer indicating potential higher depletion of $^{210}$Pb due to higher radon exhalation from the upper
405 soil layer (Table 3). However, the $^{238}$U:$^{226}$Ra ratio over all seasons is also significantly higher in the upper
406 soil layer compared to the lower soil layer (Table 3). This indicates that also other processes determine
407 the radionuclide fractionation in the soil as discussed in section 3.1.

408 In addition, no interpretations could be made related to the seasonal variability of radionuclides in
409 moss, roots or above ground tree compartments due to the limited amount of samples and/or inability
410 to reach the detection limit. Further discussions will therefore relate to the average radionuclide
411 content in soil, moss or different tree parts calculated with the combined measurements from all the
412 seasonal sampling campaigns. The soil measurements presented in Table 3 were used for the
413 calculation of transfer factors to moss and pine trees.

414 3.3.2 Radionuclide distribution in pine trees

415 When evaluating the distribution of $^{238}$U between pine tree compartments, we found that $^{238}$U was
416 mainly retained in the roots of the trees and no measurable amount could be found in the above
417 ground tree compartments (Table 4). It is indeed known that, although plant dependent, roots serve
418 as natural translocation barrier for U resulting in much lower U activity concentrations in the shoots

compared to the roots (Ebbs et al., 1998; Popic et al., 2020; Straczek et al., 2010; Vanhoudt et al., 2011). The high retention of U in tree roots has also been reported in the study by Thiry et al. (2005) in which the root compartment accounted for 99.3 % of the U budget in 35-year-old Scots pine trees grown on a revegetated U-mining heap. Chabaux et al. (2019) also reported limited cycling of U and Th by vegetation when studying the impact of trees on the U/Th and Ra/Ba budgets in forest ecosystems.

A similar pattern as for $^{238}$U could be observed for $^{226}$Ra, which was also primarily retained in the roots with low translocation to the above ground tree parts (Table 4). The transfer factors for $^{226}$Ra in roots, needles and twigs were in line with the values for *Pinus pinea* grown on uranium mill tailings in Portugal as presented by Madruga et al. (2001). In addition, the transfer factor for $^{226}$Ra in needles and twigs ($(1.4 \pm 0.3) \times 10^{-3}$) was slightly lower compared to the transfer factors for foliage of *Pinus syslvestris* trees grown on a uranium mill tailings waste pile, ranging between $(2.3 \pm 0.2) \times 10^{-3}$ and $(7.5 \pm 0.6) \times 10^{-3}$, as reported by Strok et al. (2011). However, these results suggest similar uptake and translocation of $^{226}$Ra to pine tree needles.

Although $^{226}$Ra and $^{210}$Pb transfer factors were similar to each other for the whole tree, results showed higher translocation of $^{210}$Pb from the roots to the above ground tree parts such as bark and needles and twigs (Table 4). Charro and Moyano (2017) also reported higher transfer factors for $^{210}$Pb compared to $^{226}$Ra in different tissues of vegetation (e.g. *Pinus pinaster* and *Quercus pyrenaica*) grown on a U mining-impacted soil in Central-West of Spain. As pine trees promote acidification of the soil surface, this will influence the regulation of radionuclide uptake and distribution in pine trees as suggested for $^{226}$Ra and $^{210}$Pb by Charro and Moyano (2017). While Strok et al. (2011) reported highest activity concentrations of both $^{226}$Ra and $^{210}$Pb in foliage compared to wood and shoots, our results only support this pattern for $^{210}$Pb (Table 4). The $^{210}$Pb activity concentration was significantly higher in outer bark and needles and twigs compared to wood, while no significant differences were observed in $^{226}$Ra activity concentration between different above ground tree compartments (Table 4). While

444 this might be due to different transport mechanisms within the plant, this can also be attributed to
445 foliar uptake or surface contamination of $^{210}$Pb related to $^{222}$Rn exhalation from soil (IAEA, 2017).
446 Moreover, the transfer factor of $^{210}$Pb in foliage of *Pinus sylvestris* reported by Strok et al. (2011)
447 (ranging between $(4.1 \pm 0.3) \times 10^{-3}$ and $(6.4 \pm 0.5) \times 10^{-3}$) was lower compared to the transfer factor for
448 needles and twigs in our study ($(1.7 \pm 0.2) \times 10^{-2}$) (Table 4).

449 Similar to $^{210}$Pb, the $^{210}$Po activity concentrations in >1 year-old needles and twigs and outer bark were
450 significantly higher than the $^{210}$Po activity concentration in wood (Table 4). Although uptake by and
451 distribution within plants has been reported to be different for these radionuclides, $^{210}$Po distribution
452 could also be controlled by its parent $^{210}$Pb considering the life span of the forest (IAEA, 2017).
453 However, transfer of $^{210}$Po to the roots and whole tree was more comparable to $^{238}$U transfer and as
454 such lower in comparison to $^{226}$Ra and $^{210}$Pb (Table 4). The latter results are contradictory to the
455 transfer factors (or concentration ratios) used within the ERICA tool in which $^{210}$Po transfer to trees is
456 considered comparable to $^{210}$Pb transfer (Brown et al., 2008). Care has to be taken when trying to
457 explain this divergent result due to the limited number of root samples analysed for $^{210}$Pb and $^{210}$Po.
458 When only the spring results are compared for $^{210}$Pb and $^{210}$Po in tree compartments, no immediate
459 indication is present to assume significant differences in activity concentrations between $^{210}$Pb and
460 $^{210}$Po (Table 4).

461 It has been discussed by Sheppard (2005) that unless on-site data are significantly different from
462 generic data, the generic data should be considered suitable and on-site measurements should not be
463 used exclusively. However, transfer factors for vegetation grown on waste heaps (containing naturally
464 occurring radionuclides) from the phosphate industry and especially $CaF_2$ sludge are limited or non-
465 existing. In our study, the measured radionuclide concentrations in the different environmental
466 compartments are narrowly distributed as expected considering the small sampling and monitoring
467 area. Kaasik et al. (2020) showed that, based on the data collected in our study, on-site transfer factors
468 for the $CaF_2$ waste deposit differ for $^{238}$U and $^{226}$Ra from the data used in classic compilations such as

469 IAEA 479 (IAEA, 2014), making the use of generic IAEA concentration ratios not conservative for our
470 specific case. It indicates that the radionuclide measurements in soil and vegetation specifically grown
471 on $CaF_2$ sludge are a valuable complementation to the generic concentration ratios for specific
472 contamination scenarios which was also emphasised by Sheppard (2005).

473 3.3.3 Radionuclide distribution in mosses

474 Our results showed higher $^{238}U$ accumulation in moss compared to pine trees even if moss was only in
475 contact with the topsoil of the upper soil layer (0-20 cm) containing less $^{238}U$ compared to the deeper
476 soil layers which were also in contact with the pine tree roots (Table 4 and 5). Mosses grown on
477 Norwegian sites with enhanced legacy or natural radioactivity also exhibited higher $^{238}U$ concentration
478 or higher transfer factors than other plant species (Popic et al., 2011, Popic et al., 2020). In addition,
479 the lowest $^{238}U$ transfer factors were reported for trees (birch, pine, spruce), based on the $^{238}U$ activity
480 concentration in leaves or needles (Popic et al., 2011, Popic et al., 2020). Also in our study, the
481 calculated $^{238}U$ transfer factor for mosses ($(7.8 \pm 1.6) \times 10^{-2}$) was slightly higher compared to the $^{238}U$
482 transfer factor for pine trees ($(2.0 \pm 0.2) \times 10^{-2}$) (Tables 4 and 5). Moreover, the calculated soil-to-moss
483 transfer factors were also slightly higher than those reported by Popic et al. (2020) which ranged from
484 0.01 to 0.04, depending on the sampling site.

485 Bioacculumation of the $^{238}U$ progeny ($^{226}Ra$, $^{210}Pb$, $^{210}Po$) in moss was higher compared with pine trees
486 (Tables 4 and 5). Our data demonstrated a $^{226}Ra$ transfer factor for moss comparable to that of $^{238}U$, in
487 accordance with previous studies reporting similar transfer factors for $^{238}U$ and $^{226}Ra$ (Popic et al.,
488 2020). However, our observed transfer factors for $^{210}Pb$ and $^{210}Po$ were higher than for $^{238}U$ and $^{226}Ra$
489 (Table 5). Indeed, Popic et al. (2020) also reported soil-to moss transfer factors for $^{210}Po$ being 1 to 2
490 orders of magnitude higher compared to $^{238}U$. Also within the ERICA tool, higher transfer factors for
491 lichen and bryophytes were applied for $^{210}Pb$ and $^{210}Po$ (2.60 Bq $kg^{-1}$ (fresh mass) per Bq $kg^{-1}$ soil (dry
492 mass)) compared to $^{238}U$ and $^{226}Ra$ (0.91 and 0.71 Bq $kg^{-1}$ (fresh mass) per Bq $kg^{-1}$ soil (dry mass),
493 respectively) (Brown et al., 2008). Our results showed a $^{210}Pb$:$^{210}Po$ activity ratio in the 0-20 cm soil

494 layer (calculated based on the summer samples) of 0.99, indicating secular equilibrium for those
495 radionuclides in contrast to the $^{238}U$:$^{226}Ra$ and $^{226}Ra$:$^{210}Pb$ ratios as discussed in section 3.1. The
496 $^{210}Pb$:$^{210}Po$ activity ratio for moss was also around unity (1.01) (calculated based on the spring samples),
497 indicating secular equilibrium.

498 High activity concentrations in the biomass can be due to the ability of hyalocysts and pores on moss
499 leaves to trap small particles containing radionuclides from air depositions making mosses ideal
500 biomonitors to detect atmospheric pollution (Corisco et al., 2017, Galhardi et al., 2017). Higher transfer
501 factors for $^{210}Pb$ and $^{210}Po$ could therefore reflect the accumulation of these radionuclides from the
502 atmosphere following the decay of radon after exhalation from the soil and subsequent deposition
503 onto mosses and other vegetation or from atmospheric dust deposition (Sheppard et al., 2005;
504 Vandenhove et al., 2009b). Although the dominant pathway by which mosses accumulate nutrients
505 and pollutants is through wet or dry deposition on their leaves, several studies indicate that the soil
506 can also be a source of nutrients and pollutants which can be absorbed by the leaves or leaf bases that
507 are in contact with the soil (Glime, 2017). This makes it difficult to assess the relative contributions of
508 uptake from the soil and foliar transfer to the total $^{210}Pb$ and $^{210}Po$ bioaccumulation by vegetation.
509 Nonetheless, in addition to their primary role as biomonitor for atmospheric pollution, mosses are also
510 considered important indicators on radionuclide mobility in the soil-plant interface (Corisco et al.,
511 2017; Glime, 2017).

## 4. Conclusions

The $CaF_2$ sludge on the site was found to be covered by a more organic layer resulting from litter and decomposition of organic material. Lower radionuclide activity concentrations were found in this top 20 cm layer compared to the deeper sludge layers. The unfavourable sludge characteristics such as clay texture and high pH, combined with the presence of both radiological and chemical pollutants, was reflected in the poor health of the Scots pine trees. Due to the low activity concentrations of the radionuclides in the pore water, labile solid-liquid distribution coefficients needed to be experimentally derived for $^{238}U$, stable Pb and Ba (as analogue for $^{226}Ra$) through batch adsorption-desorption tests using sludge from the site and $CaCl_2$ as liquid phase. Acidification near the root zone was mimicked using a citric acid – sodium citrate buffer resulting in much lower $K_d$ values for $^{238}U$ and Pb. These results bear a significant implication for modelling, in that realistic $K_d$ values should be used when representing the transport of radionuclides in the soil-root interface with the transport equation, and if the root acidification process is not taken into account, the transfer of radionuclides to the vegetation could be significantly underestimated.

While there was no seasonal variation in the $^{238}U$:$^{226}Ra$ ratio for the soil (top 20 cm layer) or sludge (below 20 cm), the $^{226}Ra$:$^{210}Pb$ ratio in sludge (below 20 cm) was significantly lower in winter compared to spring which might be at least partially attributable to seasonal changes in radon exhalation from the soil. This is also an important finding for modelling, pointing as it does to the fact that the transfer factor is not a factor as conventionally understood, but a varying quantity.

The higher $^{226}Ra$:$^{210}Pb$ ratio in the upper soil layer compared to the lower sludge layer also suggested radon exhalation as potential driver in radionuclide distribution in the soil and sludge. However, the increase in the $^{238}U$:$^{226}Ra$ ratio from sludge to upper soil layer also indicated the involvement of other radionuclide dispersion processes. This points at the need to incorporate into models the mechanism of radon exhalation and entrapment of the radon daughters by the foliage, as well as possible internal influx of radon into the tree via the root system.

Pine tree roots serve as natural translocation barrier for $^{238}U$, $^{226}Ra$, $^{210}Pb$ and $^{210}Po$ as these radionuclides were mainly retained in the roots with low translocation to the above ground tree parts. $^{210}Pb$ and $^{210}Po$ mainly accumulated in outer bark, needles and twigs and to a lesser extent in tree wood. This has implications for radiological assessment. The dispersion of $^{238}U$ and $^{226}Ra$ by tree needles swept by wind must by necessity be very limited, but the fall of tree bark and needles may provide a small but quantifiable impact of $^{210}Pb$ and $^{210}Po$ to the terrestrial biota inhabiting the litter beneath the tree canopies.

Furthermore, $^{238}U$ and its progeny were highly accumulated in mosses present on the site with higher transfer factors for $^{210}Pb$ and $^{210}Po$ compared to $^{238}U$ and $^{226}Ra$. This might be related to different bioaccumulation mechanisms and/or extra atmospheric deposition of $^{210}Pb$ related to radon exhalation from the soil with ingrowth of $^{210}Po$. Future research can elucidate the relative importance of the soil-plant interaction pathway and the interception pathway (driven by radon exhalation from the soil) to the bioaccumulation of $^{210}Pb$ and $^{210}Po$ in mosses and define the specific role mosses can play as indicators for long-term exposure to $^{238}U$ and its progeny.

This study contributed to the general effort to acquire site specific data and gain more in-depth knowledge of processes determining radionuclide mobility and bioavailability in soil. More specifically, it contributed to an improved understanding on what site specific data needs to be used to model the long-term influence of vegetation on radionuclide dispersion in forest ecosystems.

***Acknowledgements***

The work presented in this manuscript has been conducted in the context of the TERRITORIES project, which is part of the CONCERT project. This project has received funding from the Euratom research and training programme 2014-2018 under grant agreement No 662287.

The authors would like to thank Jean Wannijn, Robin Nauts, May Van Hees and Benjamin Maris from the Belgian Nuclear Research Centre (SCK CEN) for their valuable help in preparing the seasonal samples and characterising the soil. The authors also appreciate the advice from Dr. Nathalie Impens (SCK CEN) regarding the $K_d$ determinations and the help from Dr. Johan Paridaens (SCK CEN) for the visualisation of the dose rate measurements. We are also thankful to Dr. Jürgen Claesen from SCK CEN for his help and advice regarding the statistical analyses. The authors are particularly grateful to Prof. Dr. Caroline Vincke (Université catholique de Louvain, Belgium) for her advice when selecting the forest plot. Finally, the authors would like to thank the site owners for facilitating scientific research activities at the study site.

This publication reflects only the author's views. The information and views expressed therein are exclusively those of the authors. The European Commission is not responsible for any use that may be made of the information it contains.

***References***


Bonczyk M. (2013) A determination of the concentration level of lead $^{210}$Pb isotope in solid samples for the assessment of radiation risk occurring in coal mines. Journal of Sustainable Mining 12, 1-7.

Brown J.E., Alfonso B., Avila R., Beresford N.A., Copplestone D., Pröhl G., Ulanovsky A. (2008) The ERICA Tool. Journal of Environmental Radioactivity 99, 1371-1383.

Chabaux F., Stille P., Prunier J., Gangloff S., Lemarchand D. Morvan G., Négrel J., Pelt E., Pierret M.-C., Rihs S., Schmitt A.-D., Trémolières M., Viville D. (2019) Plant-soil-water interactions : Implications from U-Th-Ra isotope analysis in soils, soil solutions and vegetation (Strengbach CZO, France). Geochimica et Cosmochimica Acta 259, 188-210.

Charro E., Moyano A. (2017) Soil and vegetation influence in plants natural radionuclides uptake at a uranium mining site. Radiation Physics and Chemistry 141, 200-206.

Corisco J.A.G., Mihalík J., Madruga M.J., Prudêncio M.I., Marques R., Santos M., Reis M. (2017) Natural radionuclides, rare earths and heavy metals transferred to the wild vegetation covering a phosphogypsum stockpile at Barreiro, Portugal. Water, Air and Soil Pollution 228:235.

Degryse F., Smolders E., Parker D.R. (2009) Partitioning of metals (Cd, Co, Cu, Ni, Pb, Zn) in soils: concepts, methodologies, prediction and applications – a review. European Journal of Soil Science 60, 590-612.

Duquène L., Tack F., Meers E., Baeten J., Wannijn J., Vandenhove H. (2008) Effect of biodegradable amendments on uranium solubility in contaminated soils. Science of the Total Environment 391, 26-33.

Dwyer L.M., Stewart D.W., Balchin D. (1988) Rooting characteristics of corn, soybeans and barley as function of available water and soil physical characteristics. Canadian Journal of Soil Science 68, 121-132.

Ebbs S.D., Brady D.J., Kochian L.V. (1998) Role of uranium speciation in the uptake and translocation of uranium by plants. Journal of Experimental Botany 49, 1183-1190.

Endo I., Ohte N., Iseda K., Tanoi K., Hirose A., Kobayashi N.I., Murakami M., Tokuchi N., Ohashi M. (2015) Estimation of radioactive 137-cesium transportation by litterfall, stemflow and throughfall in the forests of Fukushima. Journal of Environmental Radioactivity 149, 176-185.

EPA – Environmental Protection Agency (1999) Understanding variation in partition coefficient, $K_d$, values. Volume I: The $K_d$ model, methods of measurement, and application of chemical reaction codes. US-EPA, Washington, USA.

EPA – Environmental Protection Agency (2000) Guidance for data quality assessment. Practical methods for data analysis. US-EPA, Washington, USA.

EC – European Commission (2001) Radiation Protection 122: Practical use of the concepts of clearance and exemption – Part II: Application of the concepts of exemption and clearance to natural radiation sources.

Galhardi J.A., García-Tenorio R., Francés I.D., Bonotto D.M., Marcelli M.P. (2017) Natural radionuclides in lichens, mosses and ferns in a thermal power plant and in an adjacent coal mine area in southern Brazil. Journal of Environmental Radioactivity 167, 43-53.

Gall J.E., Boyd R.S., Rajakaruna N. (2015) Transfer of heavy metals through terrestrial food webs: a review. Environmental Monitoring and Assessment 187, 201-221.

Gielen S., Vives i Batlle J., Vincke C., Van Hees M., Vandenhove H. (2016) Concentrations and distributions of Al, Ca, Cl, K, Mg and Mn in a Scots pine forest in Belgium. Ecological Modelling 324, 1-10.

Glime J. M. (2017) Nutrient relations: requirements and sources. Chapt. 8-1. In: Glime J.M. Bryophyte ecology. Volume 1. Physiological ecology. Ebook sponsored by Michigan Technological University and the International Association of Bryologists. http://digitalcommons.mtu.edu/bryophyte-ecology/

618 Goor F., Thiry Y. (2004) Processes, dynamics and modelling of radiocaesium cycling in a
619 chronosequence of Chernobyl-contaminated Scots pine (*Pinus sylvestris* L.) plantations. Science of the
620 Total Environment 325, 163-180.

621 Helmisaari H.S. (1995) Nutrient cycling in Pinus sylvestris stands in eastern Finland. Plant and Soil 1,
622 327-336.

623 Hinsinger P., Plassard C., Tang C., Jaillard B. (2003) Origins of root-mediated pH changes in the
624 rhizosphere and their responses to environmental constraints: a review. Plant and Soil 248, 43-59.

625 IAEA (2002) Modelling the migration and accumulation of radionuclides in forest ecosystems. Report
626 of the forest working group of the biosphere modelling and assessment (BIOMASS) programme, theme
627 3. International Atomic Energy Agency, Vienna.

628 IAEA (2009) Quantification of radionuclide transfer in terrestrial and freshwater environments for
629 radiological assessments. IAEA- TECDOC-1616. International Atomic Energy Agency, Vienna.

630 IAEA (2010) Technical Reports Series No. 472: Handbook of parameter for the prediction of
631 radionuclide transfer in terrestrial and freshwater environments. International Atomic Energy Agency,
632 Vienna.

633 IAEA (2013) Safety Reports Series No. 78: Radiation protection and management of NORM residues in
634 the phosphate industry. International Atomic Energy Agency, Vienna.

635 IAEA (2014) Modelling approaches for management and remediation at NORM and nuclear legacy
636 sites. Final report of working group 2 of EMRAS II Topical Heading: Reference approaches for human
637 dose assessment. Final version as submitted to the IAEA September 2014. International Atomic Energy
638 Agency, Vienna.

639 IAEA (2017) Technical Reports Series No. 484: The environmental behaviour of polonium. International
640 Atomic Energy Agency, Vienna.

641 ISO (1998) ISO 11277:1998 International Standard: Soil quality – Determination of particle size
642 distribution in mineral soil material – Method by sieving and sedimentation.

643 ISO (2010) ISO 11929:2010 Determination of the characteristic limits (decision threshold, detection
644 limit and limits of the confidence interval) for measurements of ionizing radiation – Fundamentals and
645 application.

646 Kaasik M., Mora J.C., Vives i Batlle J., Vanhoudt N., Tkaczyk A.H. (2020) Journal of Environmental
647 Radioactivity 222, no. 106315.

648 Karstens U., Schwingshackl C., Schmithüsen D., Levin I. (2015) A process-based $^{222}$radon flux map for
649 Europe and its comparison to long-term observations. Atmospheric Chemistry and Physics 15, 12845-
650 12865.

651 Li K.Y., Boisvert J.B., De Jong R. (1999) An exponential root-water-uptake model. Canadian Journal of
652 Soil Science 79, 333-343.

653 Li K.Y., De Jong R., Boisvert J.B. (2001) Comparison of root-water-uptake models. In: Sustaining the
654 Global Farm: Selected papers from the 10th Int. Soil Conservation Organization Meeting, West
655 Lafayette, IN, Purdue University and USDA-ARS National Soil Erosion Research Laboratory, pp. 1112-
656 1117.

657 Li K.Y., De Jong R., Coe M.T., Ramankutty N. (2006) Root-water-uptake based upon a new water stress
658 reduction and an asymptotic root distribution function. Earth Interactions 10, 1-22.

659 López-Coto I., Mas J.L., Bolivar J.P. (2013) A 40-year retrospective European radon flux inventory
660 including climatological variability. Atmospheric Environment 73, 22-33.

661 OECD (2000) OECD 106 Guideline for the testing of chemicals: Adsorption – desorption using a batch
662 equilibrium method.

Madruga M.J., Brogueira A., Alberto G., Cardoso F. (2001) $^{226}$Ra bioavailability to plants at the Urgeiriça uranium mill tailings site. Journal of Environmental Radioactivity 54, 175-188.

Magdziak Z., Gasecka M., Waliszewska B., Zborowska M., Mocek A., Cichy W.J., Mazela B., Kozubik T., Mocek-Plociniak A., Niedzielski P., Golinski P., Mleczek M. (2020) The influence of environmental condition on the creation of organic compounds in *Pinus sylvestris* L. rhizosphere, roots and needles. Trees - https://doi.org/10.1007/s00468-020-02046-y

Mason W.L., Alía R. (2000) Current and future status of Scots pine (*Pinus sylvestris* L.) forests in Europe. Investigación Agraria: Sistemas y Recursos Forestales 1, 317-335.

Paridaens J., Vanmarcke H. (2008) Radiological impact of almost a century of phosphate industry in Flanders, Belgium. Health Physics 95, 413-424.

Popic J.M., Salbu B., Strand T., Skipperud L. (2011) Assessment of radionuclide and metal contamination in a thorium rich area in Norway. Journal of Environmental Monitoring 13, 1730-1738.

Popic J.M., Oughton D.H., Salbu B., Skipperud L. (2020) Transfer of naturally occurring radionuclides from soil to wild forest fora in an area with enhanced legacy and natural radioactivity in Norway. Environmental Science: Processes and Impacts 22, 350-363.

R Development Core Team (2011) R: a language and environment for statistical computing. R Foundation for Statistical Computing, Vienna.

Rhoades, J. D. (1982) Soluble salts pg. 167-179. In: Page A. L. et al. (ed.) Methods of soil analysis: Part 2: Chemical and microbiological properties. Monograph Number 9 (Second Edition). ASA, Madison, WI.

Sheppard S.C. (2005) Transfer parameters – Are on-site data really better? Human and Radiological Risk Assessment 11, 939-949.

Sheppard S.C., Sheppard M.I., Ilin M., Thompson P. (2005) Soil-to-plant transfers of uranium series radionuclides in natural and contaminated settings. Radioprotection 40, S253-S259.

686 Straczek A., Duquene L., Wegrzynek D., Chinea-Cano E., Wannijn J., Navez J., Vandenhove H. (2010)
687 Differences in U root-to-shoot translocation between plant species explained by U distribution in roots.
688 Journal of Environmental Radioactivity 101, 258-266.

689 Strok M., Smodis B., Eler K. (2011) Natural radionuclides in trees grown on a uranium mill tailings waste
690 pile. Environmental Science and Pollution Research 18, 819-826.

691 Thiry Y., Schmidt P., Van Hees M., Wannijn J., Van Bree P., Rufyikiri G., Vandenhove H. (2005) Uranium
692 distribution and cycling in Scots pine (*Pinus sylvestris* L.) growing on a revegetated U-mining heap.
693 Journal of Environmental Radioactivity 81, 201-219.

694 Thiry Y., Colle C., Yoschenko V., Levchuk S., Van Hees M., Hurtevent P., Kashparov V. (2009) Impact of
695 Scots pine (*Pinus sylvestris* L.) plantings on long term $^{137}$Cs and $^{90}$Sr recycling from a waste burial site in
696 the Chernobyl Red Forest. Journal of Environmental Radioactivity 100, 1062-1068.

697 Thiry Y., Tanaka T., Dvornik A.A., Dvornik A.M. (2020) TRIPS 2.0: Toward more comprehensive modeling
698 of radiocaesium cycling in forest. Journal of Environmental Radioactivity 214, no. 106171.

699 Van den Hoof C., Thiry Y. (2012) Modelling of the natural chlorine cycling in a coniferous stand:
700 implications for chlorine-36 behaviour in a contaminated forest environment. Journal of
701 Environmental Radioactivity 107, 56-67.

702 Vandenhove H., Bousher A., Jensen P.H., Jackson D., Lambers B., Zeevaert T. (1999) Investigation of a
703 possible basis for a common approach with regard to the restoration of areas affected by lasting
704 radiation exposure as a result of past or old practice or work activity – CARE. Final report for European
705 Commission DG XI Environment, Nuclear Safety and Civil Protection under contract 96-ET-006,
706 Radiation Protection 115.

707 Vandenhove H., Gil-García C., Rigol A., Vidal M. (2009a) New best estimates for radionuclide solid-
708 liquid distribution coefficients in soils. Part 2. Naturally occurring radionuclides. Journal of
709 Environmental Radioactivity 100, 697-703.

710 Vandenhove H., Olyslaegers G., Sanzharova N., Shubina O., Reed E., Shang Z., Velasco H. (2009b)
711 Proposal for new best estimates of the soil-to-plant transfer factor of U, Th, Ra, Pb and Po. Journal of
712 Environmental Radioactivity 100, 721-732.

713 Vanhoudt N., Vandenhove H., Horemans N., Martinez Bello D., Van Hees M., Wannijn J., Carleer R.,
714 Vangronsveld J., Cuypers A. (2011) Uranium induced effects on development and mineral nutrition of
715 *Arabidopsis thaliana*. Journal of Plant Nutrition 34, 1940-1956.

716 Verbeke G., Molenberghs G. (2000) Linear mixed models for longitudinal data. Springer Series in
717 Statistics.

718 Vincke C., Thiry, Y. (2008) Water table is a relevant source for water uptake by a Scots pine (*Pinus*
719 *sylvestris* L.) stand: Evidences from continuous evapotranspiration and water table monitoring.
720 Agricultural and Forest Meteorology 148, 1419-1432.

721 Ukonmaanaho L., Merilä P., Nöjd P., Nieminen T.M. (2008) Litterfall production and nutrient return to
722 the forest floor in Scots pine and Norway spruce stands in Finland. Boreal Environment Research 13B,
723 67-91.

724 Xiao C.-W., Ceulemans R. (2004) Allometric relationships for below- and aboveground biomass of
725 young Scots pines. Forest Ecology and Management 203, 177-186.

726 Yoschenko V., Takase T., Konoplev A., Nanba K., Onda Y., Kivva S., Zheleznyak M., Sato N., Keitoku K.
727 (2017) Radiocesium distribution and fluxes in the typical *Cryptomeria japonica* forest at the late stage
728 after the accident at Fukushima Dai-Ichi Nuclear Power Plant. Journal of Environmental Radioactivity
729 166, 45-55.

730

***Figure 1***

Figure 1 – Illustration of the different steps in the selection procedure of the forest plot to install the monitoring station. The red line indicates the total area of the $CaF_2$ sludge heap covered with vegetation and available for research activities. The blue lines indicate the 3 selected areas based on the spatial variability of the gamma dose rate and the presence of Scots pine trees as dominant plant species. The green surface indicates the selected area based on the general health of the Scots pine trees. The yellow star indicates the final location to characterize the soil and to follow the distribution of radionuclides in pine trees, moss and soil.

741 ***Figure 2***


742

743 Figure 2 – Spatial variability in gamma dose rate [nSv $h^{-1}$] measured 1 meter above the ground surface.

744

***Figure 3***

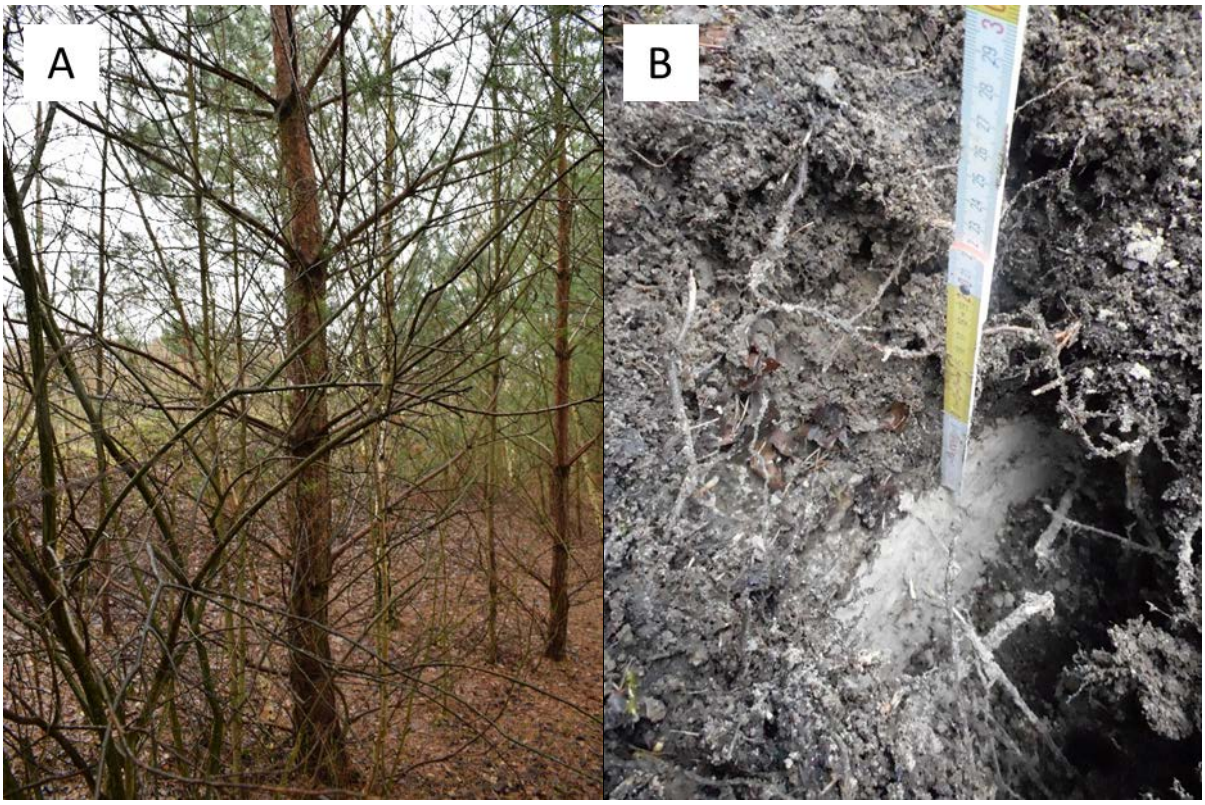


Figure 3 – Illustration of the *Pinus sylvestris* trees that grow on the site (A) and the $CaF_2$ sludge with a more organic layer on top that functions as growth substrate for the vegetation (B).

***Figure 4***

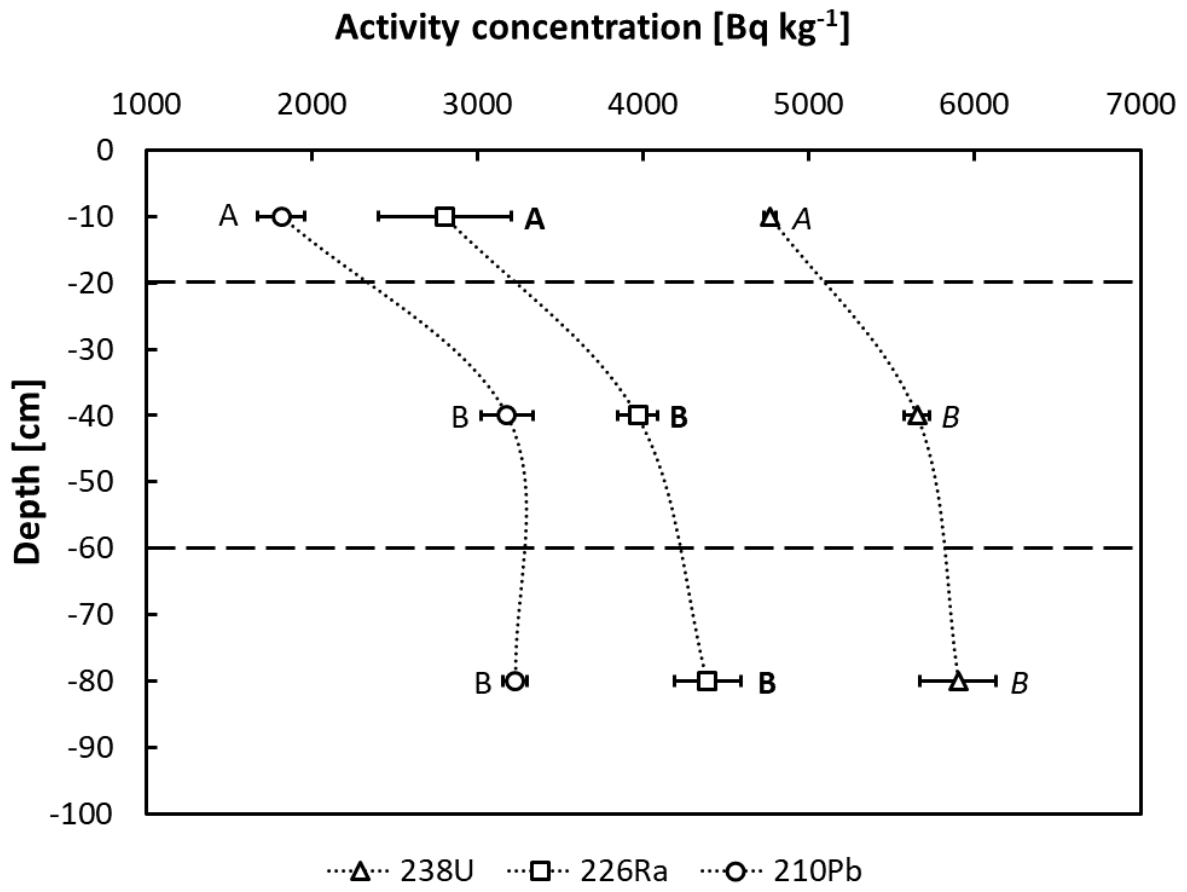


Figure 4 – Activity concentration [Bq $kg^{-1}$] of $^{238}U$, $^{226}Ra$ and $^{210}Pb$ in function of depth [cm]. Values present the average of 4 biological replicates ± SE. Samples were taken at 0-20 cm, 20-60 cm and 60-100 cm. Activity concentrations are placed on the graph at the average depths for simplicity. Different letters indicate significant differences in radionuclide activity concentration between depths ($p < 0.05$).

***Table 1***

Table 1 – Texture, total organic carbon (TOC), total inorganic carbon (TIC), field capacity (FC) and pH-$H_2O$ measured in the soil/sludge samples taken at 4 locations and 3 depths.

| Depth [cm] | Sand [%] | Silt [%] | Clay [%] | TOC [%] | TIC [%] | FC [%]* | pH-$H_2O$ |
|---|---|---|---|---|---|---|---|
| **0-20** | 10 ± 3 | 33.2 ± 0.7 | 56 ± 3 | 5.2 ± 0.8[a] | 0.37 ± 0.04[a] | 39 ± 4 | 7.3 ± 0.1 |
| **20-60** | 6.9 ± 1.2 | 30.1 ± 1.4 | 63.0 ± 0.7 | 3.61 ± 0.06[b] | 0.18 ± 0.01[b] | 34 ± 5 | 7.3 ± 0.1 |
| **60-100** | 7 ± 2 | 30.5 ± 1.4 | 63 ± 2 | 3.2 ± 0.2[b] | 0.20 ± 0.04[b] | 38 ± 3 | 7.1 ± 0.1 |

Values indicate the mean ± SE of 4 biological replicates taken at 4 locations. Different letters indicate significant differences between depth for TOC and TIC ($p < 0.05$). No significant differences were observed between depths for the other soil characteristics.

*FC = g $H_2O$/100 g soil

765 ***Table 2***

766 Table 2 – Derived solid-liquid distribution coefficients ($K_d$) for $^{238}U$, Pb and Ba (as analogue for $^{226}Ra$) in
767 a sludge sample at a depth of 60-100 cm using a batch test with additionally spiked solution.

| Element | Liquid phase | $K_d$ [L $kg^{-1}$] |
|---|---|---|
| **$^{238}U$** | 0.01 M $CaCl_2$ | (4.7 ± 0.1)E+4 |
| | 0.1 M citric acid – sodium citrate buffer (pH 5) | (3.1 ± 0.1)E+2 |
| **Pb** | 0.01 M $CaCl_2$ | (4.7 ± 0.2)E+5 |
| | 0.1 M citric acid – sodium citrate buffer (pH 5) | (1.5 ± 0.1)E+2 |
| **Ba** | 0.01 M $CaCl_2$ | (4.7 ± 0.8)E+2 |
| | 0.1 M citric acid – sodium citrate buffer (pH 5) | (4.4 ± 0.2)E+2 |

768 Values indicate the mean ± standard error of 2 replicates.

***Table 3***

Table 3 – Radionuclide activity concentrations [Bq $kg^{-1}$ DM], $^{238}U$:$^{226}Ra$ and $^{226}Ra$:$^{210}Pb$ ratios in soil/sludge samples taken at two depths.

| Season | Depth [cm] | n | $^{238}U$ [Bq $kg^{-1}$] | $^{232}Th$ [Bq $kg^{-1}$] | $^{226}Ra$ [Bq $kg^{-1}$] | $^{210}Pb$ [Bq $kg^{-1}$] | $^{210}Po$ [Bq $kg^{-1}$] | $^{238}U$:$^{226}Ra$ | $^{226}Ra$:$^{210}Pb$ |
|---|---|---|---|---|---|---|---|---|---|
| *Fall* | 0-20 | 3 | 5500 ± 120 | / | 4100 ± 400 | 2000 ± 200 | / | 1.38 ± 0.12 | 2.02 ± 0.14 |
| | 20-60 | | 6630 ± 30 | / | 4870 ± 80 | 3270 ± 150 | / | 1.36 ± 0.02 | 1.50 ± 0.07$^{ab}$ |
| *Winter* | 0-20 | 4 | 4760 ± 150 | 36 ± 9 | 2800 ± 400 | 1810 ± 40 | / | 1.46 ± 0.02 | 1.73 ± 0.06 |
| | 20-60 | | 5650 ± 160 | 44 ± 10 | 3970 ± 120 | 3180 ± 80 | / | 1.43 ± 0.01 | 1.25 ± 0.05$^{a}$ |
| *Spring* | 0-20 | 3 | 5100 ± 200 | 51 ± 4 | 3300 ± 200 | 1600 ± 40 | / | 1.55 ± 0.06 | 2.07 ± 0.11 |
| | 20-60 | | 6100 ± 200 | 67 ± 3 | 4500 ± 300 | 2630 ± 30 | / | 1.34 ± 0.08 | 1.72 ± 0.08$^{b}$ |
| *Summer* | 0-20 | 3* | 5500 ± 120 | 61 ± 7 | 3500 ± 200 | 1610 ± 15 | 1630 ± 140 | 1.56 ± 0.07 | 2.20 ± 0.14 |
| | 20-60 | | 6500 ± 100 | 65 ± 3 | 4610 ± 190 | 3000 ± 150 | 2700 ± 300 | 1.41 ± 0.04 | 1.55 ± 0.14$^{ab}$ |
| **All seasons** | 0-20 | | 5190 ± 120$^{A}$ | 47 ± 5$^{A}$ | 3400 ± 200$^{A}$ | 1770 ± 70$^{A}$ | 1630 ± 140$^{A}$ | 1.49 ± 0.04$^{A}$ | 2.00 ± 0.14$^{A}$ |
| | 20-60 | | 6170 ± 130$^{B}$ | 56 ± 6$^{B}$ | 4460 ± 120$^{B}$ | 3030 ± 80$^{B}$ | 2700 ± 300$^{B}$ | 1.39 ± 0.02$^{B}$ | 1.49 ± 0.06$^{B}$ |

Values represent the average ± SE of n biological replicates

*n = 2 for $^{232}Th$

No statistical analyses were performed to compare the radionuclide activity concentration between different seasons. Different capital letters indicate significant differences ($p < 0.05$) in radionuclide activity concentration or radionuclide ratio between the upper soil layer (0-20 cm) and the lower soil layer (20-60 cm) for the combined data of all seasons. No statistical differences were observed in the $^{238}U$:$^{226}Ra$ ratio between different seasons and this for both the top and lower soil layer. No statistical differences were observed in the $^{226}Ra$:$^{210}Pb$ ratio between seasons for the upper soil layer. Significant difference ($p < 0.05$) in the $^{226}Ra$:$^{210}Pb$ ratio between different seasons in the lower soil layer are indicated with small letters.

778 ***Table 4***

779 Table 4 – Activity concentrations [Bq $kg^{-1}$ DM] of naturally occurring radionuclides in different pine tree
780 compartments and calculation of corresponding transfer factors.

| Tree part | Season | $n_t$ | $^{238}U$ [Bq $kg^{-1}$] | $^{226}Ra$ [Bq $kg^{-1}$] | $^{210}Pb$ [Bq $kg^{-1}$] | $^{210}Po$ [Bq $kg^{-1}$] |
|---|---|---|---|---|---|---|
| **Roots** | *Fall* | 1 | 540 | 583 | 370 | / |
| | *Winter* | 0 | / | / | / | / |
| | *Spring* | 1[a] | 510 | 590 | 250 | 180 ± 20 |
| | *Summer* | 1 | 650 | 660 | 310 | / |
| **Roots** | *All seasons* | | 570 ± 40 | 610 ± 30 | 310 ± 40 | 180 ± 20 |
| **TF Roots** | | | (1.1 ± 0.1)E-1 | (1.7 ± 0.1)E-1 | (1.6 ± 0.2)E-1 | (1.0 ± 0.1)E-1 |
| **Outer bark** | *Fall* | 3 | <13 | 6 ($n_c$ = 1) | 23 ± 3 | / |
| | *Winter* | 3 | <11 | 3 ($n_c$ = 1) | 23 ± 3 | / |
| | *Spring* | 3 | <27 | <5 | 37 ± 5 ($n_c$ = 2) | 29 ± 5 |
| | *Summer* | 0 | / | / | / | / |
| **Inner bark** | *Fall* | 3 | <19 | 12 ($n_c$ = 1) | <23 | / |
| | *Winter* | 3 | <20 | 7 ($n_c$ = 1) | <30 | / |
| | *Spring* | 1[a] | <7 | 10 | <13 | 3 ± 1 |
| | *Summer* | 0 | / | / | / | / |
| **Bark** | *All seasons* | | <DL | 7 ± 2 | 18 ± 3[b] | 16 ± 5 |
| **TF Bark** | | | / | (2.0 ± 0.6)E-3 | (9.1 ± 1.5)E-3 | (9 ± 3)E-3 |
| **Wood** | *Fall* | 3 | <7 | 4 ($n_c$ = 1) | 7 ± 1 | / |
| | *Winter* | 3 | <23 | <3 | <31 | / |
| | *Spring* | 3 | <6 | 4 ($n_c$ = 1) | <12 | 6 ± 1 |
| | *Summer* | 0 | / | / | / | / |
| **Wood** | *All seasons* | | <DL | 4 ± 1 | 7 ± 1 | 6 ± 1 |
| **TF Wood** | | | / | (1.1 ± 0.3)E-3 | (3.6 ± 0.5)E-3 | (3.3 ± 0.6)E-3 |
| **Needles and twigs >1 year** | *Fall* | 3 | <36 | 6 ± 1 | 42 ± 5 | / |
| | *Winter* | 3 | <36 | 5 ($n_c$ = 1) | 46 ± 4 | / |
| | *Spring* | 3 | <22 | 4 ± 1 | 30 ± 3 ($n_c$ = 2) | 32 ± 3 |
| | *Summer* | 2 | <22 | 6 ($n_c$ = 1) | 40 ($n_c$ = 1) | / |
| **Needles and twigs <1 year** | *Fall* | 3 | <11 | 9 ± 5 ($n_c$ = 2) | 26 ± 1 | / |
| | *Winter* | 3 | <11 | 5 ($n_c$ = 1) | 26 ± 2 | / |
| | *Spring* | 1[a] | <9 | 3 ($n_c$ = 1) | <17 | 5 ± 1 |
| | *Summer* | 2 | <8 | 3 ($n_c$ = 1) | 14 ($n_c$ = 1) | / |
| **Needles and twigs** | *All seasons* | | <DL | 5 ± 1 | 33 ± 3 | 18 ± 6 |
| **TF Needles and twigs** | | | / | (1.4 ± 0.3)E-3 | (1.7 ± 0.2)E-2 | (1.0 ± 0.3)E-2 |
| **Whole tree** | *All seasons* | | 108 ± 8 | 120 ± 5 | 71 ± 8 | 42 ± 6 |
| **TF Tree** | | | (2.0 ± 0.2)E-2 | (3.4 ± 0.1)E-2 | (3.6 ± 0.4)E-2 | (2.3 ± 0.4)E-2 |

781 Values represent the average ± SE of n biological replicates; transfer factors (TF) were calculated with the activity
782 concentration in the 0-20 cm and 20-60 cm soil layer (Table 3), taking into account the relative distribution of the
783 pine tree roots in these soil layers (84 % in 0-20 cm layer and 16 % in 20-60 cm layer); $n_t$ = total number of
784 biological replicates measured; $n_c$ = number of replicates with values above the detection limit used in the
785 calculations indicated when different from $n_t$; DL = detection limit; detection limits were computed according to
786 ISO (2010) with $\alpha = \beta = 5$ %

787 [a]$n_t$ = 3 for $^{210}$Po but these are sub-samples from one biological sample
788 [b]To take the $^{210}$Pb activity concentration in the inner bark into account when calculating the total activity in the
789 bark, data below the detection limit were replaced by values equal to half of the detection limit (EPA, 2000)

790

***Table 5***

Table 5 – Activity concentrations [Bq $kg^{-1}$ DM] of naturally occurring radionuclides in moss samples and calculation of soil-to-moss transfer factors.

| **Season** | **n** | **$^{238}$U [Bq $kg^{-1}$]** | **$^{226}$Ra [Bq $kg^{-1}$]** | **$^{210}$Pb [Bq $kg^{-1}$]** | **$^{210}$Po [Bq $kg^{-1}$]** |
|---|---|---|---|---|---|
| *Fall* | 2 | 490 ± 90 | 420 ± 70 | 500 ± 10 | / |
| *Winter* | 2 | 230 ± 40 | 240 ± 40 | 340 ± 0 | / |
| *Spring* | 2 [a] | 300 ± 60 | 300 ± 100 | 355 ± 5 | 350 ± 60 |
| *Summer* | 1 | 800 | 400 | 600 | / |
| *All seasons* | 7[a] | 400 ± 80 | 340 ± 40 | 430 ± 40 | 350 ± 60 |
| **Transfer factor[b]** | | (7.8 ± 1.6)E-2 | (1.0 ± 0.1)E-1 | (2.4 ± 0.2)E-1 | (2.1 ± 0.4)E-1 |

Values represent the mean ± SE of n biological replicates

[a]n = 3 for $^{210}$Po

[b]Transfer factors were calculated with the activity concentration in the 0-20 cm soil layer (Table 3)